Added Value of Gadoxetic Acid–enhanced Hepatobiliary Phase MR Imaging in the Diagnosis of Hepatocellular Carcinoma[1]

Sung Soo Ahn, MD
Myeong-Jin Kim, MD
Joon Seok Lim, MD
Hye-Suk Hong, MD
Yong Eun Chung, MD
Jin-Young Choi, MD

Purpose: To determine the added value of hepatobiliary phase images in gadoxetic acid–enhanced magnetic resonance (MR) imaging in the evaluation of hepatocellular carcinoma (HCC).

Materials and Methods: Institutional review board approved this retrospective study and waived the informed consent. Fifty-nine patients with 84 HCCs underwent gadoxetic acid–enhanced MR examinations that included 20-minute delayed hepatobiliary phase imaging. MR imaging was performed with a 1.5-T system in 19 patients and a 3.0-T system in 40 patients. A total of 113 hepatic nodules were documented for analysis. Three radiologists independently reviewed two sets of MR images: set 1, unenhanced (T1- and T2-weighted) and gadoxetic acid–enhanced dynamic images; set 2, hepatobiliary phase images and unenhanced and gadoxetic acid–enhanced dynamic images. For each observer, the diagnostic accuracy was compared by using the area under the alternative free-response receiver operating characteristic curve (A_z). Sensitivity and specificity were also calculated and compared between the two sets.

Results: For all observers, A_z values were higher with the addition of the hepatobiliary phase. The observer who had the least experience in abdominal imaging (2 years) demonstrated significant improvement in A_z, from 0.895 in set 1 to 0.951 in set 2 ($P = .049$). Sensitivity increased with the addition of hepatobiliary phase images but did not reach statistical significance. Nine HCCs (10.7%) in six patients (10.1%) were seen only on hepatobiliary phase images.

Conclusion: Hepatobiliary phase images obtained after gadoxetic acid–enhanced dynamic MR imaging may improve diagnosis of HCC and assist in surgical planning.

[1] From the Department of Radiology, Research Institute of Radiological Science, Severance Hospital, Yonsei University College of Medicine, Shinchon-dong 134, Seodaemun-gu, Seoul 120-752, Korea (S.S.A., M.J.K., J.S.L., H.S.H., J.E.C., J.Y.C.); and Institute of Gastroenterology and Brain Korea 21 Project, Yonsei University College of Medicine, Seoul, Korea (M.J.K.). Received July 30, 2009; revision requested September 18; final revision received October 22; accepted November 3; final version accepted November 19. **Address correspondence to** M.J.K. (e-mail: *kimnex@yuhs.ac*).

The accurate identification of the number, size, and location of hepatocellular carcinomas (HCCs) is critical for planning the most appropriate therapeutic approach. In practice, however, this can be challenging due to the high prevalence of benign lesions in cirrhotic livers and the variability of imaging features in HCC depending on their differentiation. Magnetic resonance (MR) imaging, particularly contrast material–enhanced dynamic MR imaging, plays a crucial role in the accurate diagnosis of HCC (1–3). A newly developed liver-specific hepatobiliary contrast agent, gadoxetic acid disodium, is now available for use in hepatic MR examinations. Gadoxetic acid disodium is a gadolinium-based paramagnetic contrast agent that accumulates in functioning hepatocytes during the hepatobiliary phase and is cleared from the body in almost equal amounts in the urinary and biliary systems in the clinical dose range (4,5). This contrast agent combines the properties of a conventional extracellular fluid contrast agent, thus enabling dynamic perfusion imaging, and a hepatobiliary agent, allowing evaluation of delayed hepatocyte uptake and biliary excretion (6–9).

Advances in Knowledge

- Combined reading of hepatobiliary phase MR images with routine precontrast and contrast-enhanced dynamic MR images may improve diagnostic performance for the diagnosis of hepatocellular carcinoma (HCC) at gadoxetic acid–enhanced MR imaging, especially for a reviewer with least experience; the area under the alternative free-response receiver operating characteristic curve improved, from 0.895 to 0.951.
- Higher sensitivities and specificities (mean sensitivity, 89.7%; mean specificity, 92%) can be achieved with addition of hepatobiliary phase MR images, compared with those (84.9% and 89.7%, respectively) obtained with routine MR images.

Previous studies have shown that, compared with unenhanced MR images, gadoxetic acid disodium-enhanced dynamic and hepatobiliary phase imaging may provide superior detection and characterization of HCC (9–14).

To our knowledge, there have been no studies assessing the utility of the hepatobiliary phase gadoxetic acid disodium-enhanced MR imaging in addition to contrast-enhanced dynamic and T2-weighted MR imaging in the evaluation of HCC. Therefore, the purpose of this study was to determine the added value of hepatobiliary phase images in gadoxetic acid–enhanced MR imaging in the evaluation of HCC.

Materials and Methods

Patients and Standard of Reference

Our institutional review board approved this retrospective study and waived the informed consent requirement. Between May 2007 and March 2008, 59 consecutive patients (mean age, 57 years; age range, 29–75 years), 50 men (mean age, 56 years; age range, 29–75 years) and nine women (mean age, 60 years; age range 47–75 years), suspected of having HCC underwent hepatic gadoxetic acid disodium-enhanced MR imaging. There was no significant difference between age distribution by sex ($P = .3$). Forty-five patients had hepatitis B–related cirrhosis, eight had hepatitis C–related cirrhosis, two had alcoholic cirrhosis, one had Budd-Chiari disease, and the remaining three had no known underlying disease. MR examinations were performed to rule out or confirm HCC because of possible focal hepatic lesions at ultrasonography (US) or computed tomography (CT) or elevated levels of serum tumor markers (α-fetoprotein or protein induced by vitamin K absence II). A total of 113 hepatic nodules were identified in 59 patients; 34 patients had solitary lesions, 15 had two lesions, three had three lesions, four had five lesions, two had six lesions, and the remaining patient had eight lesions. Among the 113 nodules, 84 nodules were HCC.

A diagnosis of HCC was based on surgical findings ($n = 43$ nodules, 40 that were proved at pathologic examination and three that were diagnosed at intraoperative US), findings at percutaneous biopsy ($n = 5$), or a typical clinical history and tumor marker levels in combination with lipiodol uptake after transhepatic arterial chemoembolization or the progression of the disease as depicted at follow-up CT or MR imaging performed at least 1 year after initial imaging ($n = 36$). Among 45 nodules, which were confirmed pathologically, four were well-differentiated HCCs, 24 were moderately differentiated HCCs, and 17 were poorly differentiated HCCs. The diameters of the 84 HCCs ranged from 0.4 to 11 cm (mean, 2.8 cm). Among the remaining 29 nodules, six were confirmed pathologically as benign lesions associated with liver cirrhosis (cirrhosis with large cell change in three, cirrhotic liver in one, hepatitis in one, and regenerative nodule in one) and one was a confirmed hemangioma. The remaining 22 lesions were considered benign (negative) as they showed no

Implication for Patient Care

- Hepatobiliary phase images are beneficial for the improvement of diagnostic accuracy in the evaluation of HCC and should be included in gadoxetic acid–enhanced MR imaging.

Published online
10.1148/radiol.10091388

Radiology 2010; 255:459–466

Abbreviations:
A_z = area under the alternative free-response receiver operating characteristic curve
HCC = hepatocellular carcinoma

Author contributions:
Guarantors of integrity of entire study, S.S.A., M.J.K., J.Y.C.; study concepts/study design or data acquisition or data analysis/interpretation, all authors; manuscript drafting or manuscript revision for important intellectual content, all authors; approval of final version of submitted manuscript, all authors; literature research, S.S.A., M.J.K., J.S.L., J.Y.C.; clinical studies, M.J.K., J.S.L., H.S.H., Y.E.C., J.Y.C.; statistical analysis, S.S.A., M.J.K.; and manuscript editing, S.S.A., M.J.K., J.S.L.

Authors stated no financial relationship to disclose.

Table 1

Pulse Sequence Parameters for 1.5- and 3.0-T Imaging

	Respiratory-triggered Single-shot T2-weighted		Double-echo T1-weighted Gradient-echo		T1-weighted Gadoxetic Acid-enhanced	
Parameter	1.5 T	3.0 T	1.5 T	3.0 T	1.5 T	3.0 T
Matrix	288 × 230	320 × 202	256 × 256	256 ×x 208	256 × 256	256 × 192
Section thickness (mm)	7	4	7	7	2	2–2.2
Intersection gap (mm)	5	5	7.7	7.7	...	...
Repetition time (msec)	2000–3000	3580–4830	167.84–181.32	172	4.44–4.48	3.3
Echo time (msec)	80	73–81	2.3–4.6	1.22–2.5	2.17–2.19	1.18
Pixel spacing (mm)	0.742	1.094	0.742	1.484	0.742–0.781	0.742
Flip angle (degrees)	90	140	80	65	15	13
Reduction factor	2	2	1.2	2	2	2

interval change or became less conspicuous on follow-up CT or MR images for 1 year without treatment.

MR Imaging

MR imaging was performed by using a 1.5-T system (Intera Achieva; Philips Medical Systems, Best, Netherlands) in 19 patients and a 3.0-T system (TrioTim, Siemens, Erlangen, Germany; or Intera Achieva, Philips Medical Systems) in 40 patients with phased-array coils. All images were obtained in the transverse plane with a rectangular field of view of 22–24 × 38 cm, which was adjusted for each patient.

The baseline MR imaging examination for the three systems consisted of a respiratory-triggered single-shot T2-weighted sequence, double-echo T1-weighted gradient-echo sequence (in-phase and opposed-phase images), and contrast-enhanced dynamic sequence. All pulse sequence parameters are listed in detail in Table 1.

For contrast-enhanced dynamic MR imaging, 0.025 mmol per kilogram of body weight of gadoxetic acid disodium (Primovist; Bayer-Schering, Berlin, Germany) was injected as a rapid bolus and was immediately followed by a saline flush of 15–20 ml. A three-dimensional spoiled gradient-recalled-echo sequence with chemically selective fat suppression was performed during suspended respiration at 30–35 seconds (arterial phase), 65–70 seconds (portal phase), 100–120 seconds (hepatic venous phase), and 5 minutes (equilibrium phase) after the injection of the intravenous contrast agent. Additional hepatobiliary phase images were obtained at 20 minutes after injection.

Imaging Analysis

Three radiologists (J.S.L., H.S.H., Y.E.C., with 10, 7, and 2 years of experience in abdominal imaging, respectively) independently reviewed two sets of MR images in random order: set 1, unenhanced (precontrast T1- and T2-weighted images) and gadoxetic acid–enhanced dynamic images (arterial, portal, hepatic venous, and equilibrium phases); set 2, unenhanced, gadoxetic acid–enhanced dynamic, and hepatobiliary phase images. The three observers were blinded to patient history, laboratory results, findings of other imaging modalities, and final diagnosis. The interval between the reviews of the two sets of images was at least 1 month. The criteria for diagnosis of HCC were as follows (15–17): *(a)* a nodule with increased enhancement on arterial phase and washout on late venous or equilibrium phase images; *(b)* a nodule with arterial enhancement and hyperintensity on T2-weighted images; *(c)* a nodule with isointensity during contrast-enhanced dynamic study, hyperintensity on T2-weighted images, and no uptake of contrast agent on hepatobiliary phase images, or *(d)* a nodule larger than 1.5 cm with no uptake of contrast agent on hepatobiliary phase images.

Each observer recorded the possibility of HCC for each lesion by using the following four-point confidence rating scale: a score of 1, probably not HCC; a score of 2, possibly HCC; a score of 3, probably HCC; and a score of 4, definite HCC. A score of 0 was assigned retrospectively when an observer did not find a lesion documented with a standard of reference. When an observer estimated the lesion as a score of 3 or 4, the lesion was classified as positive. For exact correlation of the lesions detected by the observers with the standard of reference, we used a standardized template form composed of 12 transverse sections representing the cross-sectional anatomy of the entire liver for each examination. Each lesion was documented as accurately as possible according to size and segmental location by using the template. All images were reviewed by using a local picture archiving and communication system monitor (Centricity; GE Healthcare, Milwaukee, Wis). By comparing the scoring results from the three observers with the standard of reference, we calculated the number of true-positive, true-negative, false-positive, and false-negative lesions for each observer. Benign lesions determined by standard of reference constituted true-negative lesions.

Statistical Analysis

Statistical analyses were performed by using statistical software (SPSS, version 17.0.1, SPSS, Chicago, Ill; MedCalc, version 9.3.6.0, MedCalc Software, Mariakerke, Belgium; SAS, version 9.1.3, SAS Institute, Cary, NC). The means of age between men and women were compared by using the independent-sample *t* test. An alternative free-response receiver operating characteristic curve was fitted to each

Figure 1

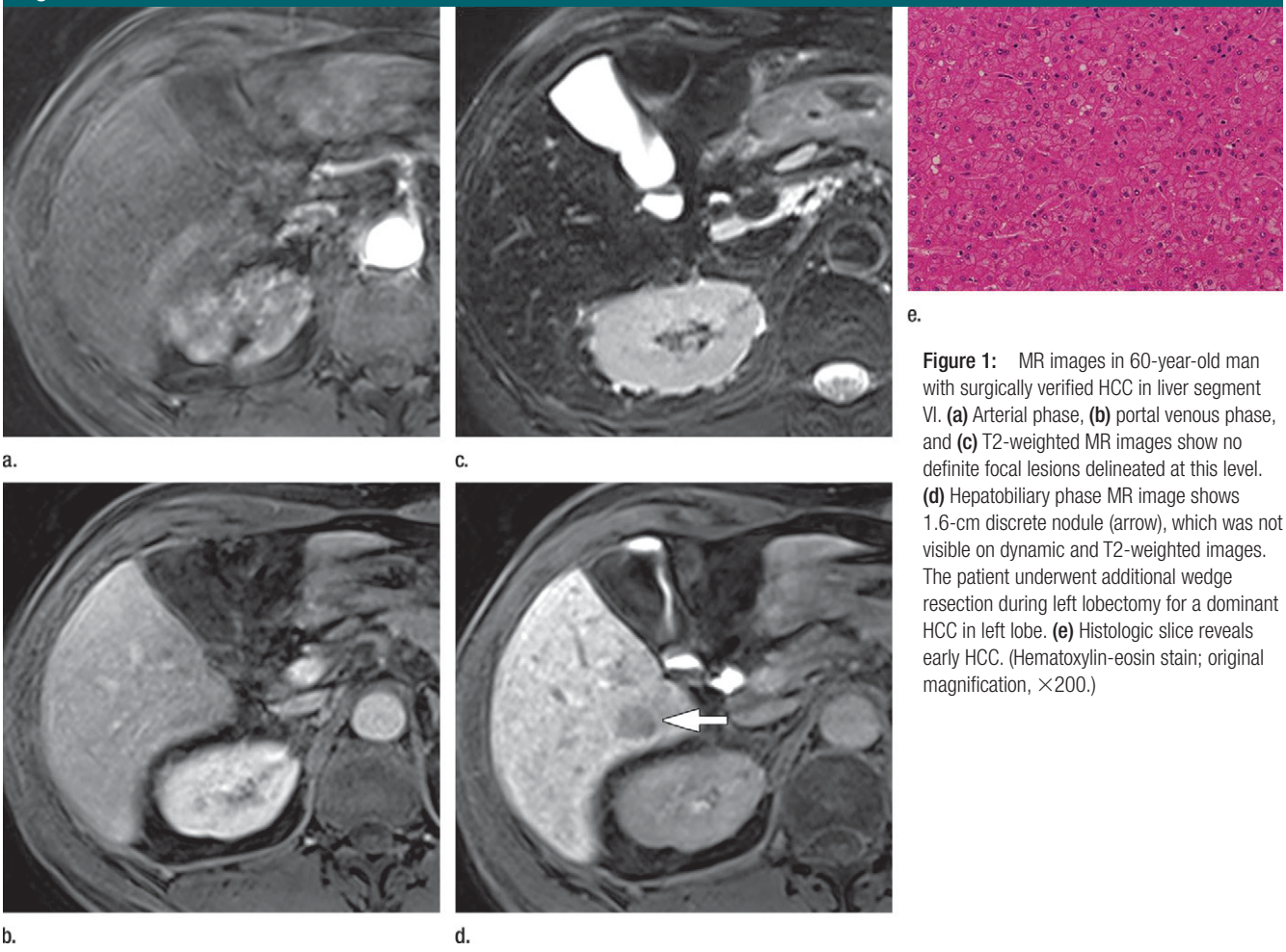

Figure 1: MR images in 60-year-old man with surgically verified HCC in liver segment VI. **(a)** Arterial phase, **(b)** portal venous phase, and **(c)** T2-weighted MR images show no definite focal lesions delineated at this level. **(d)** Hepatobiliary phase MR image shows 1.6-cm discrete nodule (arrow), which was not visible on dynamic and T2-weighted images. The patient underwent additional wedge resection during left lobectomy for a dominant HCC in left lobe. **(e)** Histologic slice reveals early HCC. (Hematoxylin-eosin stain; original magnification, ×200.)

Table 2

A_z Values for the Diagnosis of HCC for Each Observer

Observer and Mean	Set 1	Set 2	*P* Value
Observer 1	0.922	0.947	.446
Observer 2	0.901	0.910	.603
Observer 3	0.895	0.951	.049
Mean	0.906	0.936	···

Note.—The sets are defined in the Materials and Methods.

observer's confidence ratings by using maximum-likelihood estimation program (ROCKIT 0.9B; C. E. Metz, University of Chicago, Chicago, Ill, 1998). For each observer, accuracy (area under the alternative free-response receiver operating characteristic curve [A_z]) for the diagnosis of HCC was calculated and compared by using latent binomial alternative free-response receiver operating characteristic analysis. Sensitivities and specificities were calculated for the two sets of MR images for each observer. Sensitivities and specificities were also calculated according to lesion size: smaller than 1 cm, 1–2 cm, or equal to or lager than 2 cm. Sensitivities were calculated as the number of true-positive lesions divided by the total number of HCCs. Specificities were calculated as the number of true-negative lesions divided by the total number of benign nodules determined on a standard of reference. The generalized estimating equation method was used to compare the sensitivities and specificities of the two sets of MR images. We also compared the sensitivity between 1.5-T and 3.0-T MR imaging for the diagnosis of HCC for each observer. A $P < .05$ was considered to indicate a significant difference.

Results

A_z values for each observer are shown in Table 2. For all three observers, the A_z values for the combined unenhanced, gadoxetic acid–enhanced dynamic, and hepatobiliary phase images (set 2) were higher than those for the combined unenhanced and gadoxetic acid–enhanced dynamic images (set 1) (Fig 1). The observer with the least experience in abdominal imaging (2 years) showed a significant improvement in A_z, from 0.895 in set 1 to 0.951 in set 2 ($P = .049$).

The sensitivities and specificities of the two image sets for the three observers

Figure 2

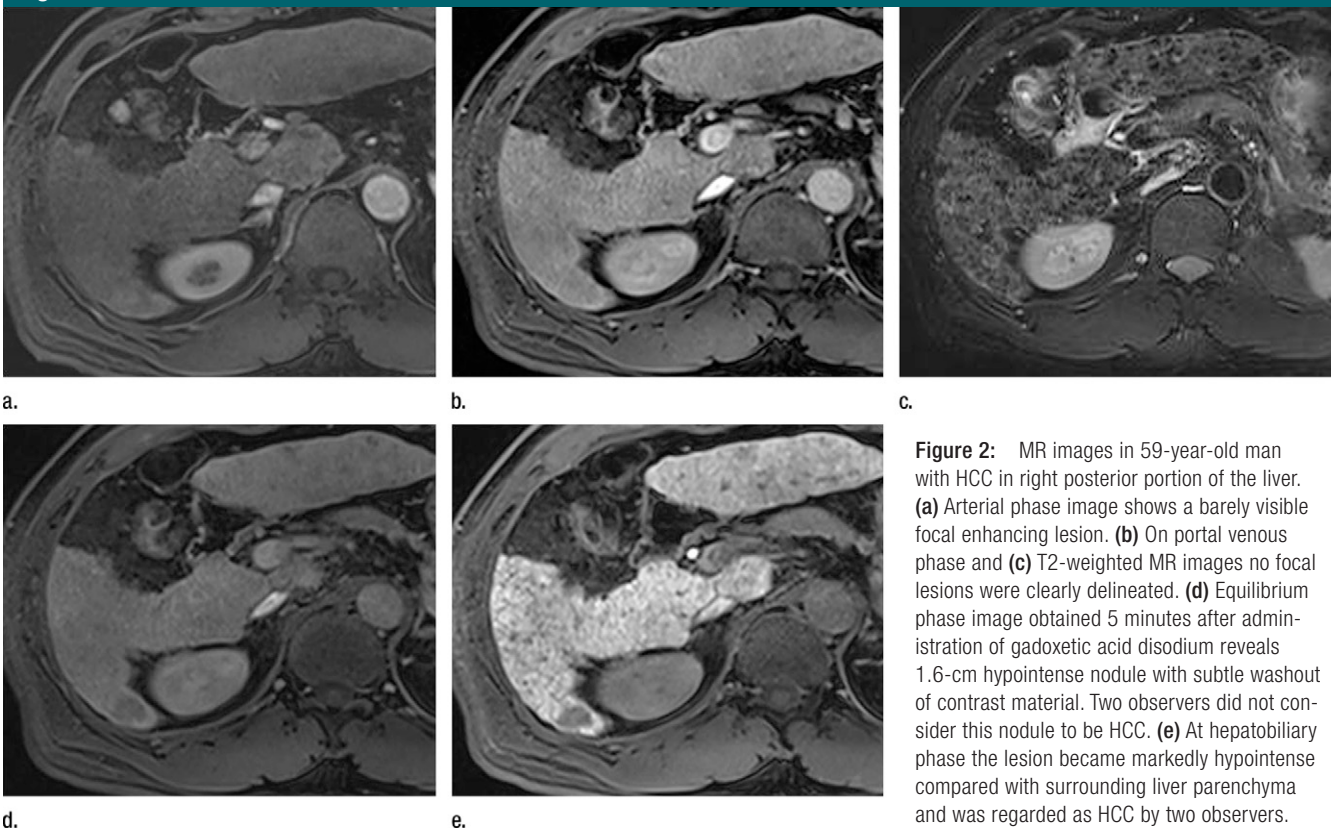

Figure 2: MR images in 59-year-old man with HCC in right posterior portion of the liver. **(a)** Arterial phase image shows a barely visible focal enhancing lesion. **(b)** On portal venous phase and **(c)** T2-weighted MR images no focal lesions were clearly delineated. **(d)** Equilibrium phase image obtained 5 minutes after administration of gadoxetic acid disodium reveals 1.6-cm hypointense nodule with subtle washout of contrast material. Two observers did not consider this nodule to be HCC. **(e)** At hepatobiliary phase the lesion became markedly hypointense compared with surrounding liver parenchyma and was regarded as HCC by two observers.

Table 3

Comparison of Sensitivities and Specificities between the Two Imaging Sets for Diagnosis of HCC

Observer and Statistic	Set 1 (%)*	Set 2 (%)*	*P* Value†
Observer 1			
Sensitivity	85.7 (72/84)	91.7 (77/84)	.057
Specificity	93.1 (27/29)	93.1 (27/29)	> .99
Observer 2			
Sensitivity	83.3 (70/84)	86.9 (73/84)	.255
Specificity	93.1 (27/29)	89.7 (26/29)	.656
Observer 3			
Sensitivity	85.7 (72/84)	90.5 (76/84)	.156
Specificity	82.8 (24/29)	93.1 (27/29)	.080

Note.—The sets are defined in the Materials and Methods.

* Numbers in parentheses were used to calculate the percentages.

† Difference between the two imaging sets.

are shown in Table 3. The sensitivities increased with the addition of hepatobiliary phase images, from 85.7% to 91.7%, 83.3% to 86.9%, and 85.7% to 90.5% for observers 1, 2, and 3, respectively (Fig 2). The increase in sensitivity with the addition of the hepatobiliary phase was observed for HCCs smaller than 1 cm in maximum diameter, with statistical significance for one observer (Table 4). There was no significant difference in terms of sensitivity between 1.5- and 3.0-T MR imaging in the diagnosis of HCC for any observer.

There were three HCCs (mean diameter, 1.1 cm) that were not appreciated by at least two observers on both image sets (Fig 3). All were depicted on hepatobiliary phase images but were not regarded as HCC by the observers because they were too small (< 1.5 cm) to be interpreted as such according to the diagnostic criteria and had no characteristic features on contrast-enhanced dynamic and T2-weighted images.

One HCC, which was interpreted as a positive lesion on contrast-enhanced dynamic and T2-weighted MR images alone, was not identified on the combined interpretation of dynamic and hepatobiliary phase images (Fig 4). The lesion was 1.5 cm in diameter and showed arterial enhancement and washout on subsequent dynamic perfusion images. However, the lesion was isointense to the surrounding parenchyma on T2-weighted and hepatobiliary phase images. There were no false-positive results identified by two or more observers on either of the two image sets.

Table 4

Comparison of Sensitivities between the Two Imaging Sets According to Lesion Size

	Observer 1 (%)			Observer 2 (%)			Observer 3 (%)		
Lesion Size (cm)	Set 1	Set 2	*P* Value*	Set 1	Set 2	*P* Value*	Set 1	Set 1	*P* Value*
<1 (*n* = 14)	9 (64.3)	10 (71.4)	0.56	7 (50.0)	9 (64.3)	.31	5 (35.7)	9 (64.3)	0.03
1–2 (*n* = 26)	21 (80.8)	25 (96.2)	0.06	21 (80.8)	20 (76.9)	.31	23 (88.5)	24 (92.3)	0.56
≥2 (*n* = 44)	42 (95.5)	42 (95.5)	> .99	42 (95.5)	44 (100)	.50	44 (100)	43 (97.7)	> .99

Note.—The sets are defined in the Materials and Methods.

* Difference in sensitivities between the two imaging sets in each group according to lesion size for each observer.

Figure 3

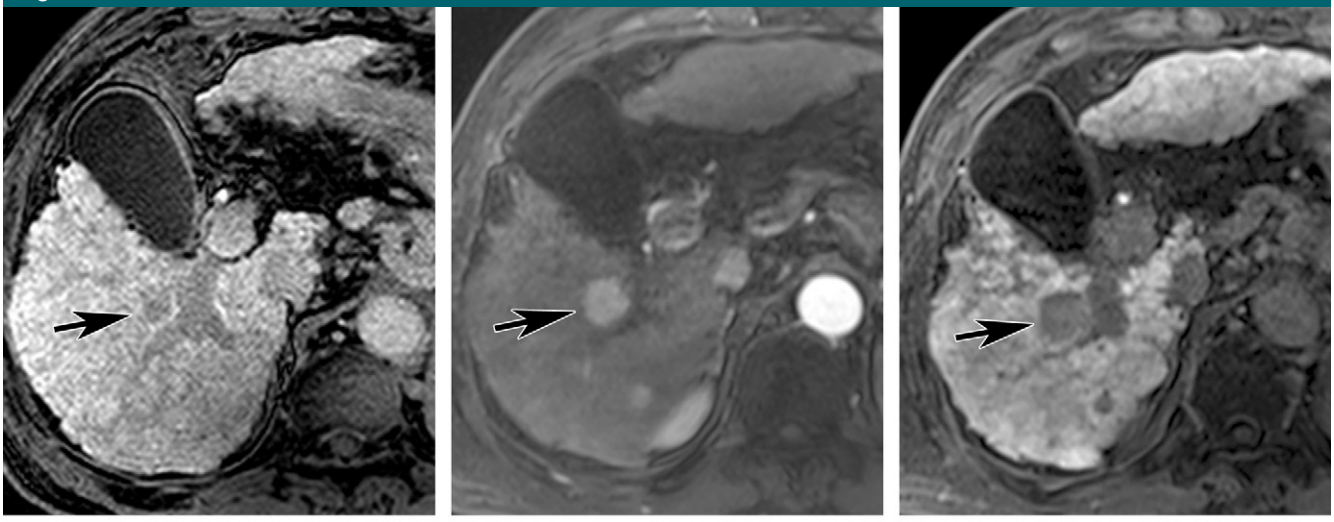

a. b. c.

Figure 3: MR images in 63-year-old man with hepatitis B–related cirrhosis. **(a)** Hepatobiliary phase image of initial MR imaging shows small hypointense nodule (arrow) that was not visible on unenhanced and dynamic images (not shown). Because of inability to exclude the possibility of HCC, follow-up was recommended. During imaging analysis, the lesion was not appreciated as HCC on precontrast and dynamic MR images because of its small size. **(b)** Arterial phase and **(c)** hepatobiliary phase MR images obtained 9 months later show that the nodule (arrow) has increased in size and shows enhancement.

Discussion

The results of our study show that modest improvement in the diagnosis of HCC may be achieved by including hepatobiliary phase images in gadoxetic acid–enhanced MR imaging. At MR imaging with use of an extracellular MR contrast agent, small HCCs frequently appear isointense on equilibrium phase images (2,18,19). In our study, however, most HCCs showing arterial enhancement revealed clear washout on late dynamic and hepatobiliary phase images, leading to an increase in diagnostic confidence. This may be attributed to the rapid and strong enhancement of the liver parenchyma on gadoxetic acid–enhanced MR images (6,8).

In our study, sensitivities increased with the addition hepatobiliary phase images for all observers. Most HCCs that were correctly diagnosed by including only the hepatobiliary phase images were small (< 2 cm) lesions. The addition of hepatobiliary phase images allowed subtle abnormalities depicted at other sequences to be better appreciated by the observers such that some lesions showing no abnormalities at other sequences were correctly interpreted as HCCs because of their clear hypointensity and size (> 1.5 cm). However, three small HCCs (< 1.5 cm) identified on hepatobiliary phase images alone were not appreciated because of their small size and absence of abnormality at other sequences. These results suggest that lesions that are visible only on hepatobiliary phase images should not be ignored or dismissed.

In our study, a small well-differentiated HCC showing typical arterial enhancement and washout at dynamic phases was found to be isointense on hepatobiliary phase images (Fig 4). The diminished conspicuity of this lesion on hepatobiliary phase images might have been related to residual hepatocyte activity within the well-differentiated lesion, permitting delayed uptake of the contrast material (20–22). Hepatic dysfunction or hyperbilirubinemia, where hepatocyte uptake of the contrast agent may be diminished, could also be another

Figure 4

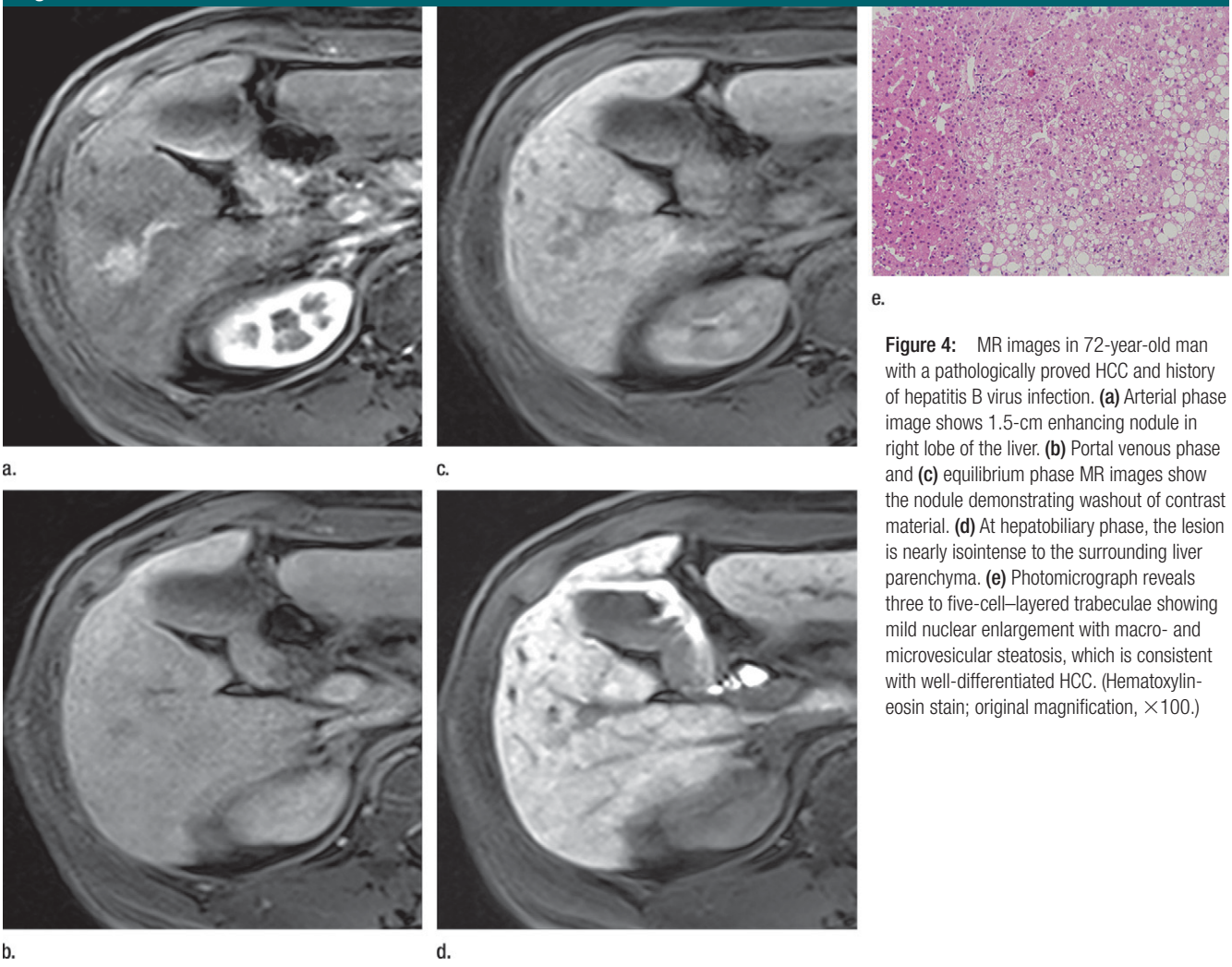

Figure 4: MR images in 72-year-old man with a pathologically proved HCC and history of hepatitis B virus infection. **(a)** Arterial phase image shows 1.5-cm enhancing nodule in right lobe of the liver. **(b)** Portal venous phase and **(c)** equilibrium phase MR images show the nodule demonstrating washout of contrast material. **(d)** At hepatobiliary phase, the lesion is nearly isointense to the surrounding liver parenchyma. **(e)** Photomicrograph reveals three to five-cell–layered trabeculae showing mild nuclear enlargement with macro- and microvesicular steatosis, which is consistent with well-differentiated HCC. (Hematoxylin-eosin stain; original magnification, ×100.)

possible cause of reduced lesion conspicuity on hepatobiliary phase images, although all false-negative cases in our study had normal billirubin level (23).

Two patients with hepatic nodules, which were identified only on hepatobiliary phase images, underwent liver resection, and early HCCs were found pathologically. Early HCC, defined as a well-differentiated HCC with a vaguely nodular appearance, lacks a fibrous capsule and often contains portal tracts (24). Because nontriadal arteries are poorly developed in early HCC, they typically fail to show a characteristic enhancement pattern and may be difficult to identify at conventional MR imaging (25–27). Early HCC has a high chance for surgical cure and a lower risk of recurrence, therefore it has a more favorable clinical outcome (28,29). These preliminary findings suggest that gadoxetic acid–enhanced MR imaging may be useful for preoperative diagnosis of early HCC.

Our study had several limitations. First, since we did not perform a biopsy of every hepatic nodule, not all lesions were confirmed pathologically. However, had we included only those lesions that were confirmed at pathologic examination, it would have led to a verification bias. Second, several small (< 1 cm) nodules seen only on hepatobiliary phase images were regarded as benign when there was no proved evidence of HCC during a follow-up period of 1 year. Given that an early HCC may take a long time to increase in size, it might be too early to determine whether those lesions were truly benign lesions. In our clinical practice, when we encounter such lesions in surgical candidates for coexisting overt HCC, we recommend resection of those lesions. Otherwise, we recommend biopsy or close follow-up depending on the lesion size and the status of the remaining liver (30). The fate of those indeterminate lesions should be documented in a long-term follow-up study. There may be potential for criticism regarding the use of either a 1.5- or a 3.0-T MR system in the present study. However, because similar results were observed with both systems, the results may be applicable for general practice using either system. Lastly, since hepatocyte

enhancement may begin before the acquisition of late dynamic phase images, the so-called equilibrium phase, it may be difficult to clearly define the value of contrast-enhanced dynamic and hepatobiliary phase images. Therefore, the improved lesion conspicuity on later dynamic phase images might have counteracted the additional benefit of the hepatobiliary phase images.

Currently, at our institution, gadoxetic acid is the first choice of a contrast agent in liver MR examinations for evaluating patients at high risk of HCC. Per our protocol, these hepatobiliary phase images are acquired at 10 and 20 minutes after the injection of contrast media. Further study may be necessary to determine the optimal imaging delay for the acquisition of hepatobiliary phase images. In summary, hepatobiliary phase images obtained after gadoxetic acid–enhanced dynamic MR imaging may assist in better diagnosis of HCC and thus may help guide treatment planning.

References

1. Bartolozzi C, Donati F, Cioni D, Crocetti L, Lencioni R. MnDPDP-enhanced MRI vs dual-phase spiral CT in the detection of hepatocellular carcinoma in cirrhosis. Eur Radiol 2000;10(11):1697–1702.
2. Yamashita Y, Mitsuzaki K, Yi T, et al. Small hepatocellular carcinoma in patients with chronic liver damage: prospective comparison of detection with dynamic MR imaging and helical CT of the whole liver. Radiology 1996;200(1):79–84.
3. Kwak HS, Lee JM, Kim CS. Preoperative detection of hepatocellular carcinoma: comparison of combined contrast-enhanced MR imaging and combined CT during arterial portography and CT hepatic arteriography. Eur Radiol 2004;14(3):447–457.
4. Weinmann HJ, Schuhmann-Giampieri G, Schmitt-Willich H, Vogler H, Frenzel T, Gries H. A new lipophilic gadolinium chelate as a tissue-specific contrast medium for MRI. Magn Reson Med 1991;22(2):233–237; discussion 242.
5. Clément O, Mühler A, Vexler V, Berthezène Y, Brasch RC. Gadolinium-ethoxybenzyl-DTPA, a new liver-specific magnetic resonance contrast agent. Kinetic and enhancement patterns in normal and cholestatic rats. Invest Radiol 1992;27(8):612–619.
6. Hamm B, Staks T, Mühler A, et al. Phase I clinical evaluation of Gd-EOB-DTPA as a hepatobiliary MR contrast agent: safety, pharmacokinetics, and MR imaging. Radiology 1995;195(3):785–792.
7. Reimer P, Rummeny EJ, Shamsi K, et al. Phase II clinical evaluation of Gd-EOB-DTPA: dose, safety aspects, and pulse sequence. Radiology 1996;199(1):177–183.
8. Vogl TJ, Kümmel S, Hammerstingl R, et al. Liver tumors: comparison of MR imaging with Gd-EOB-DTPA and Gd-DTPA. Radiology 1996;200(1):59–67.
9. Huppertz A, Balzer T, Blakeborough A, et al. Improved detection of focal liver lesions at MR imaging: multicenter comparison of gadoxetic acid-enhanced MR images with intraoperative findings. Radiology 2004;230(1):266–275.
10. Bluemke DA, Sahani D, Amendola M, et al. Efficacy and safety of MR imaging with liver-specific contrast agent: U.S. multicenter phase III study. Radiology 2005;237(1):89–98.
11. Huppertz A, Haraida S, Kraus A, et al. Enhancement of focal liver lesions at gadoxetic acid-enhanced MR imaging: correlation with histopathologic findings and spiral CT—initial observations. Radiology 2005;234(2):468–478.
12. Halavaara J, Breuer J, Ayuso C, et al. Liver tumor characterization: comparison between liver-specific gadoxetic acid disodium-enhanced MRI and biphasic CT—a multicenter trial. J Comput Assist Tomogr 2006;30(3):345–354.
13. Hammerstingl R, Huppertz A, Breuer J, et al. Diagnostic efficacy of gadoxetic acid (Primovist)-enhanced MRI and spiral CT for a therapeutic strategy: comparison with intraoperative and histopathologic findings in focal liver lesions. Eur Radiol 2008;18(3):457–467.
14. Kim SH, Kim SH, Lee J, et al. Gadoxetic acid-enhanced MRI versus triple-phase MDCT for the preoperative detection of hepatocellular carcinoma. AJR Am J Roentgenol 2009;192(6):1675–1681.
15. Choi SH, Lee JM, Yu NC, et al. Hepatocellular carcinoma in liver transplantation candidates: detection with gadobenate dimeglumine-enhanced MRI. AJR Am J Roentgenol 2008;191(2):529–536.
16. Kim YK, Kwak HS, Han YM, Kim CS. Usefulness of combining sequentially acquired gadobenate dimeglumine-enhanced magnetic resonance imaging and resovist-enhanced magnetic resonance imaging for the detection of hepatocellular carcinoma: comparison with computed tomography hepatic arteriography and computed tomography arterioportography using 16-slice multidetector computed tomography. J Comput Assist Tomogr 2007;31(5):702–711.
17. Willatt JM, Hussain HK, Adusumilli S, Marrero JA. MR Imaging of hepatocellular carcinoma in the cirrhotic liver: challenges and controversies. Radiology 2008; 247(2):311–330.
18. van den Bos IC, Hussain SM, Dwarkasing RS, et al. MR imaging of hepatocellular carcinoma: relationship between lesion size and imaging findings, including signal intensity and dynamic enhancement patterns. J Magn Reson Imaging 2007;26(6):1548–1555.
19. Hayashida M, Ito K, Fujita T, et al. Small hepatocellular carcinomas in cirrhosis: differences in contrast enhancement effects between helical CT and MR imaging during multiphasic dynamic imaging. Magn Reson Imaging 2008;26(1):65–71.
20. Grazioli L, Morana G, Caudana R, et al. Hepatocellular carcinoma: correlation between gadobenate dimeglumine-enhanced MRI and pathologic findings. Invest Radiol 2000;35(1):25–34.
21. Gabata T, Matsui O, Kadoya M, et al. Delayed MR imaging of the liver: correlation of delayed enhancement of hepatic tumors and pathologic appearance. Abdom Imaging 1998;23(3):309–313.
22. Manfredi R, Maresca G, Baron RL, et al. Delayed MR imaging of hepatocellular carcinoma enhanced by gadobenate dimeglumine (Gd-BOPTA). J Magn Reson Imaging 1999;9(5):704–710.
23. Kim T, Murakami T, Hasuike Y, et al. Experimental hepatic dysfunction: evaluation by MRI with Gd-EOB-DTPA. J Magn Reson Imaging 1997;7(4):683–688.
24. Hytiroglou P, Park YN, Krinsky G, Theise ND. Hepatic precancerous lesions and small hepatocellular carcinoma. Gastroenterol Clin North Am 2007;36(4):867–887, vii.
25. Nakashima Y, Nakashima O, Hsia CC, Kojiro M, Tabor E. Vascularization of small hepatocellular carcinomas: correlation with differentiation. Liver 1999;19(1):12–18.
26. Takayasu K, Furukawa H, Wakao F, et al. CT diagnosis of early hepatocellular carcinoma: sensitivity, findings, and CT-pathologic correlation. AJR Am J Roentgenol 1995; 164(4):885–890.
27. Lim JH, Choi D, Kim SH, et al. Detection of hepatocellular carcinoma: value of adding delayed phase imaging to dual-phase helical CT. AJR Am J Roentgenol 2002;179(1):67–73.
28. Inoue K, Takayama T, Higaki T, Watanabe Y, Makuuchi M. Clinical significance of early hepatocellular carcinoma. Liver Transpl 2004;10(2 suppl 1):S16–S19.
29. Yamamoto M, Takasaki K, Otsubo T, et al. Favorable surgical outcomes in patients with early hepatocellular carcinoma. Ann Surg 2004;239(3):395–399.
30. Bruix J, Sherman M, Llovet JM, et al. Clinical management of hepatocellular carcinoma: conclusions of the Barcelona-2000 EASL conference. European Association for the Study of the Liver. J Hepatol 2001;35(3):421–430.